Lab on a Chip

A soft microchannel decreases polydispersity of droplet generation

Journal:	*Lab on a Chip*
Manuscript ID:	LC-ART-07-2014-000871
Article Type:	Paper
Date Submitted by the Author:	24-Jul-2014
Complete List of Authors:	Pang, Yan; Beijing University of Technology, College of Mechanical Engineering & Applied Electronics Technology Kim, Hyoungsoo; Princeton University, Mechanical and Aerospace Engineering Zhaomiao, Liu; Beijing University of Technology, College of Mechanical Engineering & Applied Electronics Technology Stone, Howard; Princeton University, Mechanical and Aerospace Engineering

Cite this: DOI: 10.1039/c0xx00000x

www.rsc.org/loc

PAPER

A soft microchannel decreases polydispersity of droplet generation

Yan Pang,[a] Hyoungsoo Kim,[b] Liu Zhaomiao,[a] and Howard A. Stone*[b]

Received (in XXX, XXX) Xth XXXXXXXXX 20XX, Accepted Xth XXXXXXXXX 20XX
DOI: 10.1039/b000000x

We study the effect of softness of the microchannel on the process of droplet generation in two-phase flows in a T-junction microchannel. One side of the microchannel has a flexible thin PDMS layer, which vibrates naturally while droplets are generated; the deformation frequency coincides with the frequency of droplet formation. Furthermore, we compare the polydispersity of water-in-oil droplets formed with a microchannel with one soft wall with those formed in a conventional rigid microchannel. We show that deformation of the soft wall reduces the polydispersity in the droplet size.

Introduction

The formation and control of droplets are a significant area of development for microfabrication methods and have enabled new microfluidic applications in chemical and biological research [1-2]. One of the common structures with which to form droplets is a T-junction microchannel where two immiscible liquids intersect at the junction and discrete droplets are produced periodically. There are many studies of droplet generation focusing on the influence of flow geometry [1-6], flow conditions [1, 7], and fluid properties [1, 8], as well as organizing the data with appropriate dimensionless parameters. For example, generally, for a given geometry and fluid properties, the capillary number is the most important parameter to distinguish the regimes of drop formation. In particular, three main regimes of droplet formation have been identified as the capillary number is varied: squeezing, dripping, and jetting [2, 8-11]. In contrast, in this paper we maintain the flow conditions approximately constant so as not to significantly change the capillary number in the flow, but we influence the droplet formation process by redesigning a microchannel with one soft wall, as shown in Fig. 1 and Supplementary Movie 1. As the movie makes clear (data reported in detail below) we observe more regular droplet formation by using the channel with a soft wall.

The effects of the elastic deformation of a microchannel on the pressure drop versus flow rate relation for the case of a steady single-phase laminar flow were investigated by Gervais et al. [12]. These authors reported that for a given pressure difference the measured liquid flow rate in the deformed channel is much higher than occurs in a non-deforming channel (a model for the modified pressure drop versus flow rate relation was given also). In addition, a deforming wall has been used as a microvalve, as apparently first introduced by Unger et al. [13], who fabricated two embedded channels in polydimethylsiloxane (PDMS). By controlling the deformable wall using air pressure, the authors tuned the droplet size and droplets were produced at the same frequency as the valve was actuated [14]. In extensions of the study of [13], microvalves of various shapes have been fabricated and used in the micro-controlled systems [15], pumps [16-17] and droplet generation chips [18-19].

In this paper, we are interested in the effect of a soft wall on the process of droplet formation in a T-junction. The soft microchannel can significantly influence droplet break up as evidenced in Fig. 1. To investigate this effect, we introduce a new T-junction microchannel that has one side consisting of a thin membrane that forms a flexible soft wall. By using a confocal laser-scanning microscope, we observe the deformation of the soft microchannels. To measure the frequency of the fluctuations of the soft wall, we prepare the thin PDMS layer with a dilute distribution of fluorescent particles, which are then observed with a high-speed camera. We find that the deformation frequency is synchronized with the droplet formation sequence. Finally, we compare droplet generation in microfluidic T-junction experiments with the soft wall and the conventional rigid channel and show that the soft wall geometry provides droplets with smaller polydispersity than in the conventional rigid wall T-junction.

Materials and methods

In order to investigate multiple characteristics of droplet generation in a soft microchannel, including the size and formation frequency of droplets, as well as the deformation and vibration frequency of a soft wall, the experimental setup shown in Fig. 2(a) is used. Two straight channels merge at a right angle with two inlets and one outlet. An oil phase (perfluoropolyether oil, Fomblin 06/6, Kurt J. Lesker, USA) flows in the main channel (the *y*-direction) as the continuous phase liquid, deionized water, flows through the side channel (the *x*-direction) to be dispersed as water droplets in the junction area. A snapshot of droplet formation in the T-junction microchannel is shown in Fig. 2(b). The flow rates are controlled by syringe pumps (KD Scientific, KDS-100). The flow rate of perfluoropolyether oil is varied from 0.04 - 0.16 ml/hr while the flow rate of water is kept constant at 0.02 ml/hr. We use a non-swelling oil (perfluoropolyether oil) to prevent microchannel changes [20].

The oil has density 1880 kg·m^{-3} and dynamic viscosity 0.1147 Pa·s, and water has density 10^3 kg·m^{-3} and dynamic viscosity 10^{-3} Pa·s; the interfacial tension γ between the oil and water is about 48.3 ± 1 mN/m. The oil wets the PDMS channel.

We perform experiments in two different channels, one with one soft wall and the other where all of the walls are much less flexible. All PDMS channels are fabricated under identical conditions. To evaluate the reproducibility, all experiments are performed several times. Fig. 2(c) shows the schematic of the cross-section of the soft microchannel, where the main PDMS part with the microchannel pattern is sealed against a thin PDMS membrane that forms the bottom wall. The thin wall is made of PDMS with the ratio of 15:1 on a silicon wafer that is spin coated at 5000 RPM for 1 minute to obtain a film thickness of 17 µm. The wafer is treated by trichloro (1H, 1H, 2H, 2H-perfluorooctyl) silane (Sigma Aldrich, USA, CAS: 78560-45-9) at 110°C in a vacuum chamber for about 30 minutes. For experiments with a "rigid" microchannel, the channel is bonded on a glass slide to restrict the deformation of the bottom wall, as shown in Fig. 2(d). The two different types of microchannels have the same hydrophobicity. Furthermore, we vary the thickness of the soft wall by changing the speed of spin coating (6000 RPM for 5 µm thickness and 5500 RPM for 10 µm thickness), and so significantly influence the bending modulus of the membrane, which varies as the cube of the membrane thickness. The dimensions of the various microchannels are listed in Table A of the Supplementary Material. The Young's moduli (E) of three different soft walls were measured by using an Agilent Nano Indenter G200 and the values are listed along with the bending stiffness B in Table B of the Supplementary Material. The bending stiffness B is calculated according to the equation, $B = EI$ where I is the second moment of area; $I = t^3 w_m/12$ for a thin film of thickness t and width w_m.

To understand the dynamics in our experiments we measure the deformation frequency of the soft wall by means of a single particle detection technique. We prepare a thin PDMS layer mixed with 1 µm fluorescent particles (polystyrene Rhodamine B, Invitrogen, USA) and we measure the fluorescent signal from the particles by using a fluorescent microscope outfitted with a high-speed camera (Phantom v7.3, Vision Research, Inc.). The particles exhibit a fringe pattern that changes in time depending on the particle's position with respect to the focal plane. By taking the Fourier transform of the measured time-dependent signal we obtain the vibration frequency of the soft boundary.

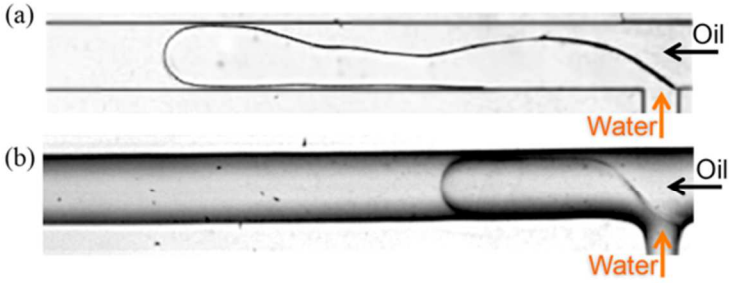

Fig. 1. Comparison of water-in-oil droplet formation in (a) the conventional rigid T-junction and (b) the soft wall T-junction, which are performed under the same experimental conditions, i.e. the same flow rates and the same sizes of microchannels. (a) A PDMS channel is constructed with a glass substrate, which represents the conventional rigid microchannel. (b) A thin PDMS layer replaces the glass substrate for the bottom substrate where deflections of the thin membrane cause small distortion of the images. Images at droplet breakup are captured from the Supplementary Movie 1.

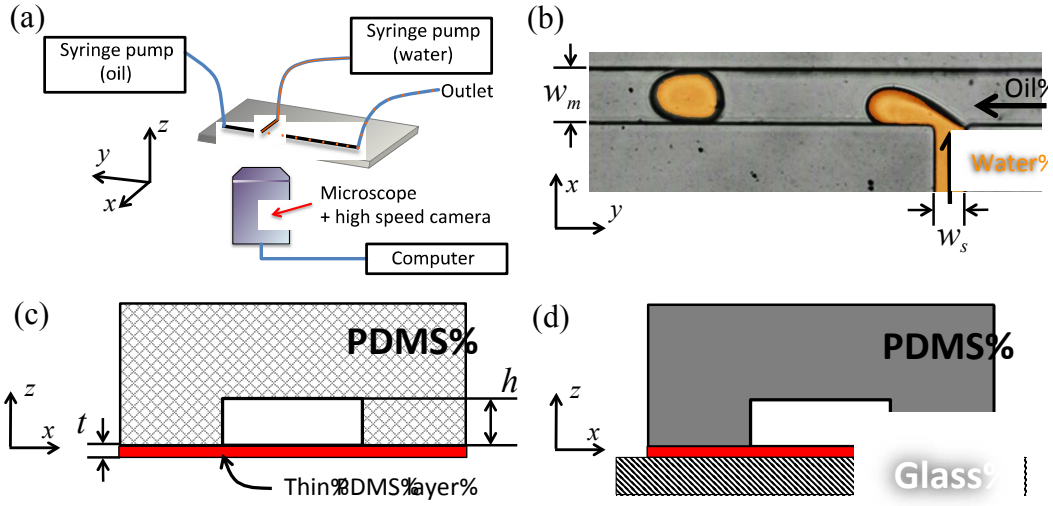

Fig. 2. Characteristics for drop formation in a microchannel with one soft wall. (a) Schematic illustration of the experimental setup for droplet generation. (b) Snapshot of droplet generation in the T-junction microchannel where w_s and w_m are, respectively, the widths of the channels of the water and oil phases. The water droplet is artificially indicated with orange. Comparison of the cross-sections between (c) the soft microchannel and (d) the rigid microchannel, where h is the channel height and t is the thickness of the thin PDMS layer.

Cite this: DOI: 10.1039/c0xx00000x

www.rsc.org/loc

PAPER

Results and discussion

We now discuss our observations of drop formation in a microchannel specially designed with one soft wall. In particular, we first document the deformation of the soft wall in two-phase flow, then we document the deformation of the soft boundary as drops are formed periodically, and finally we contrast the drop size and polydispersity for a microchannel with one soft wall as compared to the conventional much more rigid microchannel. The observed decrease in polydispersity in the softer design is the main contribution of our work.

Deformation of the soft wall of the microchannel

First, to visualize the deformation of the soft microchannel, the channel is colored by Rhodamine B (Sigma Aldrich, USA). To prepare this material, a Rhodamine B solution is pumped into the microchannels and then allowed to sit for about 1 hour. After this treatment, we measure the shape of the microchannel by using a confocal laser-scanning microscope (Leica TCS SP5, Leica Microsystems Inc.). Fig. 3 illustrates that the soft wall deforms and the cross-sectional area increases when water droplets are generated. The deformation δ increases with the microchannel's width under the same flow rate condition, as shown by comparing the typical deformations in Fig. 3(b) and (d). The maximum deformation δ values of Fig. 3(b) and (d) are 8 μm and 32 μm, respectively.

For wider membranes, the deformation is larger (contrast Fig. 3(b) and (d)). The deformation of a flexible thin membrane can be described by a spring-mass system. Then, by Hooke's law, we can approximate the deformation of the membrane, $\delta \sim F_R w_m^3 E^{-1} L^{-1} t^{-3}$, where F_R is the force acting on the membrane and L is a droplet length in the channel; we then have the spring constant $k = w_m^{-3} E L t^3$ for the thin layer [21]. From this relation, we assume that the final deformation is mainly determined by the width of the channel and the PDMS layer thickness, provided that the Young's modulus and the force acting on the wall are similar.

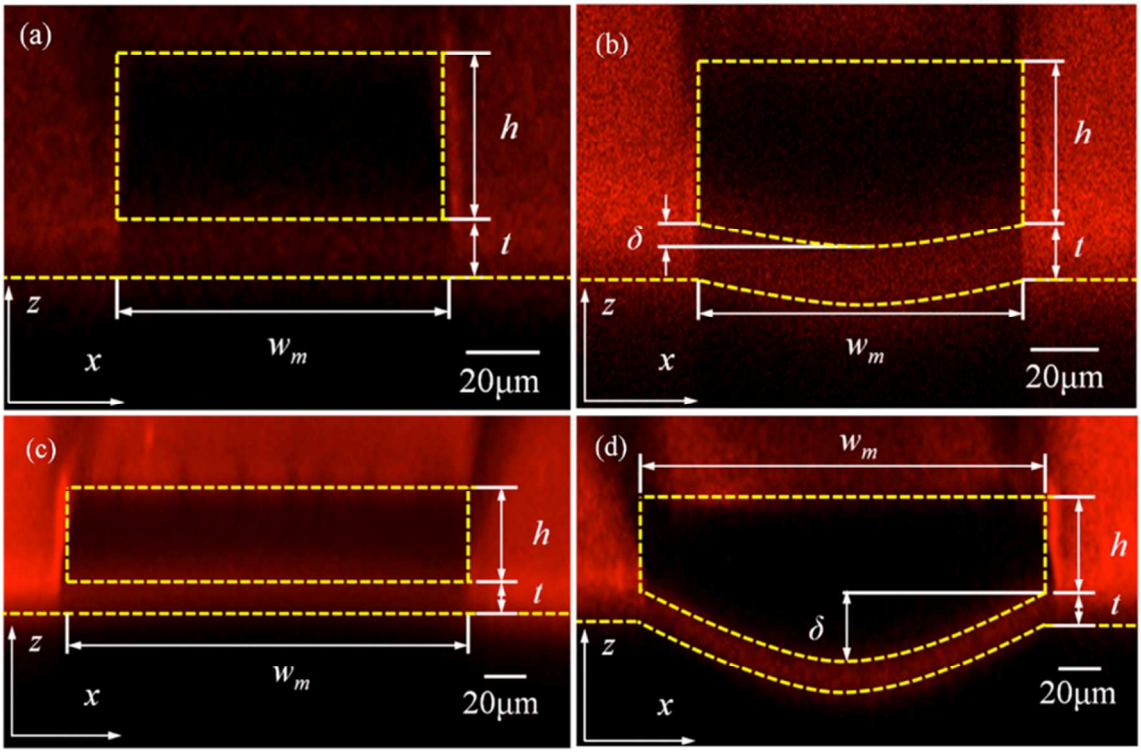

Fig. 3. Comparison of the deformations of soft microchannels where panels (a) and (c) have no flow while panels (b) and (d) have two-phase flow. The flow rate of water is Q_w = 0.02 ml/hr and for oil is Q_o = 0.04 ml/hr. The cross-section of the microchannel is measured by using a confocal laser-scanning microscope where the channel height is h = 45 μm and the thin membrane thickness is t = 17 μm. The PDMS microchannel is colored with Rhodamine B. The yellow dashed lines indicate the cross-sectional shape of the microchannel. Each microchannel has the same aspect ratio between the width of the oil phase channel and the width of the water phase channel, i.e. w_m/w_s = 2. (a) w_m = 100 μm, without flow. (b) w_m = 100 μm, with flow. (c) w_m = 200 μm, without flow. (d) w_m = 200 μm, with flow. The maximum deformation δ of the thin membrane is δ = 8 μm for (b) and δ = 32 μm for (d).

Cite this: DOI: 10.1039/c0xx00000x

www.rsc.org/loc

PAPER

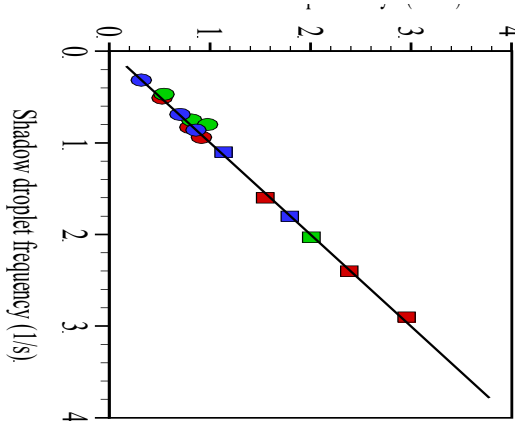

Fig. 4. Comparison of the frequency of vibration of a soft wall and the frequency of droplet generation. The different symbols represent different experiments. The solid line represents a linear fit to the experimental results.

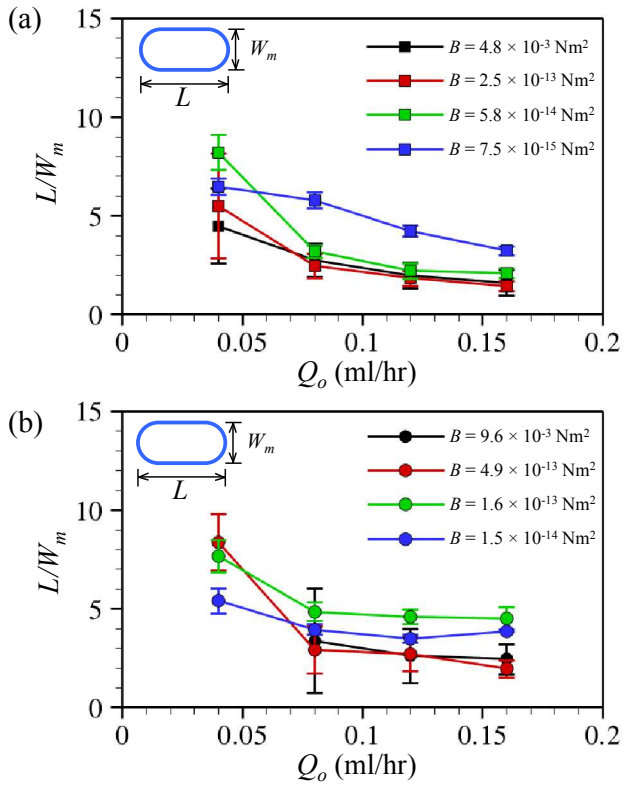

Fig. 5. Comparison of the droplet sizes measured in the soft microchannel (the red, green, and blue solid lines) and the rigid microchannel (black solid lines) by varying the oil flow rate Q_o for a fixed water flow rate Q_w = 0.02 ml/hr. The square and circle symbols represent (a) w_m = 100 μm and (b) w_m = 200 μm wide channels, respectively. Every microchannel has the same aspect ratio between the width of the oil and water phase channels, i.e. w_m/w_s = 2.

Deformation caused by droplet generation

We observe the cross-sectional shape of a channel with a deformed soft wall and find that the wall vibrates in time. In a conventional rigid microchannel, the droplet is confined and flattened by the rigid boundary, while with a soft wall the droplet flexes the elastic boundary by the pressure between the two immiscible liquids. We observe that the soft wall moves in and out of the focal plane during droplet generation. By recording the change in the particle fringe pattern inside the soft wall, we obtain the frequency. Also, the frequency of droplet generation is analyzed from high-speed droplet images. For the same experimental conditions the frequencies of wall deformation and drop formation coincide with each other, as shown in Fig. 4, which means that the soft wall is deformed by the forces associated with the droplet flows.

Droplet sizes in two different T-junctions

Under the same experimental conditions, we investigate the droplet generation process in different microchannels: soft versus rigid. The width ratio between the main channel and side channel is an important parameter in setting the droplet size and the mechanism of the droplet generation [1-6]. We maintain the same size ratio between the widths of the oil phase channel and the water phase channel, i.e. w_s/w_m = 2. To check the reproducibility of our results, we perform many experiments under the same conditions. Droplet lengths are decreased by increasing the oil flow rate, which are measured directly from the images of the droplet shadows recorded by a high-speed camera, as shown in the inset of Fig. 5 (see Supplementary Movies 2, 3, and 4 that are for case 8 ($B = 1.5\times10^{-14}$ Nm^2) and the oil flow rate has 0.04, 0.08, and 0.16 ml/hr, respectively). The droplet length is investigated by varying the oil phase flow rate in the main channel. We also examine droplet lengths in various soft microchannels that have different bending stiffnesses (see Table B of the Supplementary Material).

We examine droplet production with respect to the softness of the wall of the microchannel. Although the channels are different, in every case the droplet length L decreases as the oil flow rate, as shown by the results reported in Fig. 5. In addition, we find that as long as one wall of the channel is soft, the error bars of the droplet size distribution decrease. Thus, we next discuss the polydispersity in droplet formation.

Effect of the soft microchannel on polydispersity

The polydispersity of the generated droplet size in soft versus rigid microchannels in presented in Fig. 6. The polydispersity in droplet size is obtained as the standard deviation in droplet length relative to the average length of the droplets. In the soft microchannels, the droplet polydispersity is decreased for a wide range of oil phase flow rates. As the membrane thickness decreases, the bending stiffness decreases and we observe that the polydispersity decreases accordingly. Thus, we have provided

evidence that making the membrane softer (reducing E or the membrane thickness, both which reduce B) decreases the droplet polydispersity. For example, in case 4 (B = 7.5 ×10^{-15} Nm^2) and case 8 (B = 1.5×10^{-14} Nm^2), the polydispersity is less than 10 % for the various flow rates. In the rigid microchannel, when water droplets are formed at the T-junction, the droplets block the flow of the oil phase and then the droplet might deform due to the confinement. However, in experiments with the soft microchannel, the thin elastic wall is deformed easily as shown by the results in Fig. 3; deformation tends to relieve the confinement and leads to a lower polydispersity.

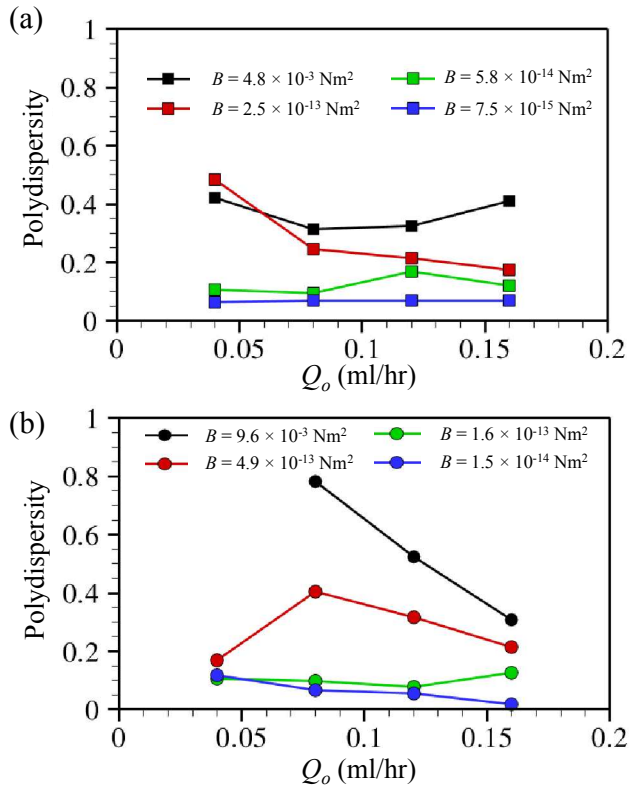

Fig. 6. Comparison of the polydispersity in droplet size for a soft microchannel (red, green, blue solid lines) and a rigid microchannel (black solid lines). The results are obtained by varying the oil flow rate Q_o for the water flow rate Q_w = 0.02 ml/hr. The square and circle symbols represent (a) w_m = 100 μm and (b) w_m = 200 μm wide channels, respectively. Every microchannel has the same aspect ratio between the widths of oil and the water phase channels, i.e. w_m/w_s = 2.

According to the literature [1-2, 8-11], at a T-junction microchannel, three distinct regimes of droplet formation - squeezing, dripping, and jetting - have been identified, which are dependent on the capillary number, $Ca = \mu Q_0/(\gamma A) = \mu U_0/\gamma$ where μ is the oil phase velocity in the main channel, U_0 is the mean velocity of the oil phase, and A is the cross-sectional area, i.e. $A = hw_m$. In particular, a critical value of the capillary number ($Ca \sim 10^{-2}$) is reported to distinguish the squeezing-to-dripping transition. In the current study, the capillary number ranges from 0.003 to 0.023 for all flows, so that the capillary numbers are in the critical range for the squeezing-to-dripping transition. Above a capillary number $Ca > 10^{-2}$, the viscous shear stress are significant and then a droplet can break up aided by the strong shear flow (i.e. dripping) while generating a droplet, as shown in Fig. 1(a) and the top row of the Supplementary Movie 1. However, in the soft wall T-junction, the flexible wall is deformed while the water phase is injected and the increase of the cross-sectional area has been observed by the confocal laser-scanning microscope measurements (see Fig. 3). By increasing the cross-sectional channel area (e.g. see Fig. 3(b) and (d)), the shear stress, $\tau \approx \mu Q_0/A\varepsilon$ where ε is the gap between the droplet interface and the wall of the channel [1], is temporally decreased and the squeezing dynamics assists breakup of the water droplets, directly at the T-junction, rather than downstream, as shown in Fig. 1(b) and the bottom row of the Supplementary Movie 1. Quantitatively, the cross-sectional area of the soft microchannel is increased and then the mean velocity ($U_0 = Q_0/A$) of the oil phase is decreased due to deformation of the flexible thin PDMS wall: the local capillary number at the junction is temporally decreased by 30 % between case 5 (B = 9.6 ×10^{-3} Nm^2) and case 6 (B = 1.6 ×10^{-13} Nm^2) while the flow rate is constant.

In addition, the soft wall provides another advantage that increases the effective surface tension force $F_\gamma \approx \gamma h(t)$ [1-2], which is related to the stabilizing effect of surface tension against breakup. By increasing the channel height as the soft wall is deformed under the flow, the effective contact line between the two immiscible liquids is increased (see the schematic of Fig. A in the Supplementary Material). In fact, when the droplet is generated at the soft wall T-junction, the multiphase flow causes more deformation than does a comparable single-phase flow. From the single particle fringe detection results, we validated that the particle signal is synchronized with the droplet formation, which means the droplet flow bends the membrane further by the capillary pressure of a droplet. Due to this effect, the effective surface tension force F_γ is temporarily increased, which produces an additional stabilizing effect against breakup and further highlights benefits of using a soft wall in droplet-based microfluidic devices. Although we have explained qualitatively the droplet formation mechanism in the soft wall T-junction, further detailed investigation and numerical simulations will be required to obtain a better understanding.

Conclusions

We have demonstrated that droplet formation with lower polydispersity in drop size can be produced in a soft wall T-junction compared with a microchannel with conventional rigid walls. We have designed and tested experimental systems to study the deformation of the soft wall during droplet formation. By using a confocal laser-scanning microscope, we measured the deformed cross-section of the microchannel and observed that the soft wall is deformed by the pressure of droplet flow. By placing fluorescent particles inside the soft wall, the deformation frequency of the soft wall is obtained by detecting the change in the particle fringe patterns, which are recorded by a high-speed camera. Comparing droplet shadowgraphy measurements and soft wall vibrations, we determined that the frequency of deformation of the soft wall coincides with the droplet formation frequency. Due to the flexible wall, when the droplets form, the stresses at the liquid-liquid interface are reduced temporarily as compared to the case of drop formation in a confined rigid

channel and, as a consequence, we find that the soft wall reduces the polydispersity in the droplet size. We believe that this design consideration may be useful rather generally in the many areas utilizing droplet microfluidics.

Acknowledgements

The authors thank members of the Complex Fluids Group at Princeton University for many fruitful discussions during the progress of this work. We are grateful for the support of grants No. 11072011 from the National Natural Science Foundation of China as well as China Scholarship Council. We thank the NSF for partial support from CBET-1132835 and the DOE for support via grant no. DE-SC0008598.

Notes and references

[a] *College of Mechanical Engineering & Applied Electronics Technology, Beijing University of Technology, Beijing, China.*
[b] *Department of Mechanical and Aerospace Engineering, Princeton University, NJ 08544, USA. E-mail: hastone@princeton.edu*

† Electronic Supplementary Information (ESI) available: [details of any supplementary information available should be included here]. See DOI: 10.1039/b000000x/

1 P. Garstecki, M. J. Fuerstman , H. A. Stone and G. M. Whitesides, *Lab on a Chip*, 2006, **6**(3), 437-446.
2 G. F. Christopher, N. N. Noharuddin, J. A. Taylor and S. L. Anna, *Physical Review E,* 2008, **78**(3), 036317.
3 J. Husny and J. J. Cooper-White, *Journal of Non-Newtonian Fluid Mechanics*, 2006, **137**(1), 121-136.
4 J. H. Xu, G. S. Luo, G. G. Chen and J. D. Wang, *Journal of Membrane Science*, 2005, **266**(1), 121-131.
5 G. F. Christopher and S. L. Anna, *Journal of Physics D: Applied Physics*, 2007, **40**(19), R319.
6 A. Gupta, and R. Kumar, *Physics of Fluids*, 2010, **22**(12), 122001.
7 X. B. Li, F. C. Li, J. C. Yang, H. Kinoshita, M. Oishi, and M. Oshima, *Chemical Engineering Science*, 2012, **69**(1), 340-351.
8 S. M. S. Murshed, S. H. Tan, N. T. Nguyen, T. N. Wong and L. Yobas, *Microfluidics and Nanofluidics*, 2009, **6**(2), 253–259.
9 G.T. Vladisavljević, N. Khalid, M. A. Neves, T. Kuroiwa, M. Nakajima, K. Uemura, S. Ichikawa and I. Kobayashi, *Advanced Drug Delivery Reviews*, 2013, **65**(11), 1626-1663.
10 S. Van Der Graaf, T. Nisisako, C. G. P. H. Schroen, R. G. M. Van Der Sman and R. M. Boom, *Langmuir*, 2006, **22**(9), 4144-4152.
11 M. De Menech, P. Garstecki, F. Jousse and H. A. Stone, *Journal of Fluid Mechanics*, 2008, **595**, 141-161.
12 T. Gervais, J. El-Ali, A. Günther, and K. F. Jensen, *Lab on a Chip*, 2006, **6**(4), 500-507.
13 M. A. Unger, H. P. Chou, T. Thorsen, A. Scherer and S. R. Quake, *Science*, 2000, **288**(5463), 113-116.
14 S. K. Hsiung, C. T. Chen, and G. B. Lee, *Journal of Micromechanics and Microengineering*, 2006, **16**(11), 2403.
15 W. H. Grover, A. M. Skelley, C. N. Liu, E. T. Lagally and R. A. Mathies, *Sensors and Actuators B: Chemical*, 2003, **89**(3), 315-323.
16 W. H. Grover and R. A. Mathies, *Lab on a Chip*, 2005, **5**(10),1033–1040.
17 A. M. Stockton, M. F. Mora, M. L. Cable and P. A. Willis, *Sensors and Actuators B: Chemical*, 2013, **177**, 668-675.
18 Y. H. Lin, C. H. Lee and G. B. Lee, *Journal of Microelectromechanical Systems*. 2008, **17**(3), 573-81.
19 H. W. Wu, Y. C. Huang, C. L. Wu and G. B. Lee, *Microfluidics and Nanofluidics*, 2009, **7**(1), 45-56.
20 R. Dangla, F. Gallaire, and C. N. Baroud, *Lab on a Chip*, 2011, **10**(21), 2972-2978.
21 N. T. Nguyen and S. T. Wereley, Fundamentals and Applications of Microfluidics. Artech House, 2002.

